The combination of elevated CO₂ and warmer temperature reduces photosynthetic capacity without diluting leaf N concentration in Amur linden (*Tilia amurensis* Rupr.)

Lei Wang[1,2]*, Jinping Zheng[2,3], Gerong Wang[2,3] and Qing-Lai Dang[2]*

[1] Jiyang College, Zhejiang A&F University, 77 Puyang Road. Zhuji, Zhejiang 311800, China

[2] Faculty of Natural Resources Management, Lakehead University, 955 Oliver Road, Thunder Bay, Ontario P7B 5E1, Canada

[3] Forestry College, Beihua University, 3999 Binjiang East Road, Jilin, Jilin 132013, China

 *Corresponding author. E-mail : rockyking@163.com (L.W.); qdang@lakeheadu.ca (Q.D.)

Abstract

Elevated CO_2 and warmer temperatures represent the future environmental conditions in the context of global change. A good understanding of plant response to their combined effects is, therefore, critically important for predicting future plant performance. This study investigated the photosynthetic acclimation of amur linden (*Tilia amurensis* Rupr.) seedlings (current year, about 60 cm tall), a shade-tolerant tree species in the temperate broadleaf deciduous forest, to the combination of current CO_2 concentration and temperature (CC) and the combination of the predicted future CO_2 concentration and temperature (FC). The results show that FC promoted aboveground growth, but reduced photosynthetic capacity (V_{cmax}: maximum rate of RuBP carboxylation and J_{max}: maximum photosynthetic electron transport rate). However, the photosynthetic rate measured under the corresponding growth CO_2 concentration was still higher under FC than under CC. FC depressed the photosynthetic limiting transition point (C_{i-t}, A_{n-t}) from Rubisco carboxylation to RuBP regeneration, i.e., A_{n-t} decreased without a change in C_{i-t}. FC did not change leaf N concentration but increased the total leaf N content per tree and photosynthetic nitrogen utilization efficiency. This suggests that N utilization, rather than photosynthetic capacity, may play an important role in the acclimation of the species to future climatic conditions. This study provides new insights into the photosynthetic acclimation of amur linden and can be used to predict its possible performance under future climatic conditions.

INTRODUCTION

CO_2 elevation and global warming will inevitably continue in the foreseeable future (Dong et al. 2023; Dusenge et al. 2020). The rising CO_2, warming temperature, and nitrogen deposition are considered the most relevant environmental conditions for global change (Kim et al. 2021; Zheng et al. 2023). The combination of elevated CO_2 and warmer temperature appears to be a continuous driver of environmental change (Maxwell et al. 2022) and controls the bioavailability of soil organic nitrogen and plant responses to global change (Hu et al. 2023; Liu et al. 2023).

There have been numerous reports in the literature on plant acclimation to increasing CO_2 and temperature (Ainsworth and Long 2021; Dusenge et al. 2019; Huang et al. 2021). It is generally believed that elevated CO_2 can reduce photosynthetic capacity, foliar nitrogen concentration, and stomatal conductance (Chavan et al. 2019; Dang et al. 2021; Kurepin et al. 2018), while warmer temperature increases leaf-to-air vapor pressure deficit, specific leaf area, respiration rate and decreases J_{max}/V_{camx} (Dusenge et al. 2021; Liang et al. 2013; Smith and Keenan 2020). However, there are inconsistent conclusions about the combined effects of elevated CO_2 and temperature on plants (Way et al. 2015). Some studies report synergistic effects (Ainsworth and Long 2021; Apgaua et al. 2019), while others find antagonistic effects (Dusenge et al. 2020; Noyce et al. 2019). While there are extensive studies on the effects of single factors, the ecophysiological significance of single-factor studies is limited under natural environmental conditions where multiple factors change simultaneously (Dong et al. 2023; Kizildeniz et al. 2021).

Climate change continues to impact forests, particularly boreal and temperate forests (Dusenge et al. 2020; Kurepin et al. 2018; Liu et al. 2023). Although temperate forests are one of the most well-studied forest type, it is still not well understood how well broadleaved deciduous tree species will be able to cope with the rapidly increasing CO_2 concentration and climate warming (Helcoski et al. 2019). Climate change is altering fundamental physiological processes such as photosynthesis and respiration which affect tree growth and survival, and trees will need to acclimate to new climatic conditions physiologically and/or morphologically to persist at their current sites (Kramer et al. 2020). Furthermore, past studies on climate change are primarily focused on the responses of commercial tree species, such as *Poplar*, *Betula*, *Quercus*, and *Maple*, to individual climate or environment factors (Dang et al. 2021; Gardner et al. 2021; Way et al. 2015). In reality, however, multiple factors change simultaneously, for example, the

elevation of CO_2 is coupled with warming. There are generally variations in response among different tree species and such variations will influence the responses of tree communities (Raizada et al. 2009; Smith et al. 2013). Therefore, a good understanding of the responses of different tree species, both commercial and non-commercial, to the combination of elevated CO_2 and warming may serve as a basis for assessing forest responses to climate change (Pastore et al. 2019).

Genus *Tilia* represents a major group of shade-tolerant tree species in temperate broadleaved deciduous forests (Aasamaa and Aphalo 2017). These species provide not only an important source of nectar but also timber and ornamental trees (Baczewska-Dąbrowska et al. 2022; Kang et al. 2021). *Tilia* has very different ecophysiological traits than other temperate broadleaved deciduous tree species. For example, most of the photosynthates in *Tilia* are used in the synthesis of new tissues or lipids (triacylglycerols) stored in the wood (Keel et al. 2007) while the increased photosynthates in other broadleaved deciduous tree species are mainly used for the growth of new tissues in the aboveground organs (Wang et al. 2022). While the effects of elevated CO_2 on the physiological traits of *Tilia* species have been examined (Li et al. 2019), the photosynthetic responses of *Tilia* species to a combination of elevated CO_2 and higher temperature, a scenario of climate change, still have not been experimentally investigated. This study investigated the photosynthetic and growth responses of amur linden seedlings to a combination of elevated CO_2 and warmer temperatures. Since the availability of light is the primary limit to trees growing under shade, the ability to expand leaf area is critical for the survival and growth of shade tolerant tree species. We test the hypothesis that amur linden will increase photosynthate production under elevated CO_2 and warmer temperature and that the increase in photosynthate production will lead to an increase in the total leaf area and biomass production.

MATERIALS AND METHODS

Plant materials and treatments

Amur linden (*Tilia amurensis* Rupr.) seeds were collected from 10 trees about 100m apart from each other in a natural forest in the Changbai Mountain forest region, China (42.1 °N; 127.5°E). Seeds were germinated in germination trays filled with a mixture of vermiculite and peat moss (1:1 in v:v) (Sun Gro® Peat Moss Grower Grade Green and Vermiculite Premium Grade, Sun

Gro Horticulture, Agawam, United States of America) in a greenhouse at Lakehead University (Thunder Bay campus, ON. Canada). The environmental conditions during the 3-week germination period were 25ºC/16ºC day/night temperatures and 16 h photoperiod.

Three weeks after germination, seedlings were transplanted into 3.5 L plastic pots filled with a vermiculite-peat moss mixture (1:1 in v:v). There were two combination treatments: the current climate condition (CC: 400 µmol mol^{-1} CO_2 and current temperature) and the predicted future climate condition (FC: 750 µmol mol^{-1} CO_2 and elevated temperature (current + 4 ℃)). Each of the two combination treatments were independently replicated twice. The treatments were randomly assigned to four independent greenhouses (2 treatments × 2 replicates per treatment = 4). There were 12 seedlings in each treatment replicate. High-pressure sodium lamps (Signify Canada Ltd. 281 Hillmount Road Markham, ON, L6C 2S3) were used to supplement the natural light when the flux density of natural light was below 500 µmol m^{-2} s^{-1}. The day/night temperatures for the CC treatment were 25ºC/16ºC while those for the FC were 29ºC/20ºC. The photoperiod was 16h for both treatments. 25ºC/16ºC temperatures and 16-h period are optimal for the photosynthesis and growth of the species. The seedlings were irrigated every two days to the drip point (about 500 ml water) and fertilized twice a week using a fertilizer solution of 150-60-150 µmol mol^{-1} N-P-K with 4 ml L^{-1} Micro pH Perfect Fertilizer (Advanced Nutrients, 8687 Melrose Ave, Suite G320, West Hollywood, CA 90069). Each greenhouse is equipped with a stirring fan to ensure uniformity in environmental conditions at different locations. Furthermore, the positions of seedlings were rotated weekly within the same greenhouse. The design and orientation of the four greenhouses are identical and the environmental conditions of each greenhouse were independently monitored and controlled using an Argus Titan Environment-control system (Argus Control Systems Ltd, Vancouver, BC, Canada). The elevated [CO_2] was achieved by a CO_2 generator (model GEN-2E; Custom Automated Products Inc., Riverside, California, USA).

Biomass and leaf nitrogen measurements

The height of all the seedlings was measured after 3-month treatment. The seedlings were then removed from the pot and separated into roots, stems, and leaves. The total leaf area for each seedling was scanned and estimated using the Regent WinFolia system (Regent Instruments Inc., Quebec City, QC, Canada). The roots were washed off the growing media. All the materials

were then oven-dried at 75°C for 48 h to determine the total biomass, leaf mass, shoot mass, and root mass. The root/shoot ratio, leaf mass ratio (LMR = leaf mass / total biomass), shoot mass ratio (SMR = stems mass / total biomass), and root mass ratio (RMR= root mass / total biomass) were calculated.

Leaf N concentration was analyzed using the dry combustion method with a CNS-2000 (LECO Corp., St. Joseph, MI, USA) at the Lakehead University Centre for Analytical Services. The leaf area-based N concentration (N_{area}, g m^{-2}) was calculated by dividing the mass-based leaf N concentration (N_{mass}, mg g^{-1}) by the specific leaf area. The total leaf nitrogen content per plant (N_{leaf}, mg plant^{-1}) was calculated as the product of N_{mass} (mg g^{-1}) and total leaf mass per tree. The photosynthetic nitrogen use efficiency (PNUE, µmol g^{-1} N s^{-1}) was the ratio of net photosynthesis rate (A_n) and N_{area} (A_n/N_{area}).

A/C$_i$ curves measurement and calculations of V_{cmax} and J_{max}

Three seedlings were randomly selected from each replicate of each treatment after two months of treatments for measuring photosynthetic CO_2 response curves (A/C$_i$ curves). The measurements were taken on the first fully expanded leaf from the top at 400, 300, 200, 150, 100, 50, 400, 500, 750, 900, 1100, and 1300, µmol mol^{-1} CO_2 (C_a) using a PP-Systems CIRAS-3 Portable Photosynthesis System equipped with a PLC3 Universal Leaf Cuvette with automatic environment control and a built-in CFM-3 Chlorophyll Fluorescence Module (PP Systems International, Inc. Amesbury, MA, USA). The first measurement was taken at the treatment CO_2 for both treatments. The measurement conditions were set at 25°C air temperature, 50% RH, and 800 µmol m^{-2} s^{-1} PAR. It generally took 2-5 minutes to achieve a stable reading at each CO_2.

The maximum electron transport rate (J_{max}, µmol m^{-2} s^{-1}) and maximum Rubisco carboxylation rate (V_{cmax}, µmol m^{-2} s^{-1}) of each sample leaf were estimated using the Plantecophys fitaci function of the R package (Duursma 2015). The initial slope of the A/C$_i$ curve (linear part) was taken as the apparent carboxylation efficiency (ACE), and the CO_2 compensation point (CCP_{aci}) was estimated from the x-axis intercept of the A/C$_i$ curve. The transition point (C_{i-t}, A_{n-t}) of the photosynthesis limitation from Rubisco carboxylation to RuBP regeneration was obtained using the findCiTransition function of plantecophys R (Duursma 2015).

The Laisk dataset was measured at 200, 150, 100, and 50 µmol mol^{-1} [CO_2] and 300, 150, and 75 µmol m^{-2} s^{-1} PAR for estimating intercellular CO_2 compensation point (C_i*) and daytime

respiration (R_d) (G.D. Farquhar et al. 1980). The rate of electron transport (J) was estimated from the chlorophyll fluorescence measurement. The variable J method was employed to calculate the mesophyll conductance g_m (Peter et al. 1992), which assumed that C_i^* (intercellular CO_2 compensation point) was equal to Γ^* (CO_2 compensation point in the chloroplast) according to Momayyezi's protocol (Momayyezi and Guy 2017).

Statistical analyses

The effects of CO_2 and temperature combined treatment were analyzed using ANOVA. The treatment was considered as fixed effects while replicates were considered as random effects in the analysis, and the sampling unit (tree seedling) was nested within each treatment replicate. Before the ANOVA, the normality distribution and homogeneity of the data were examined using probability plots for residuals. Log transformation was used when the distribution was not normal. The physiological and biomass parameters with a significant difference were subjected to Principal Component Analysis (PCA) using the PCA function from the FactoMineR package. All the analyses were performed using the R Package 4.2.1.

RESULTS

Growth and photosynthetic traits

Seeding biomass, height, total leaf area per tree, and shoot mass ratio were greater under FC (Table 1, Figs. 1). V_{cmax}, J_{max}, g_m and R_d were lower in FC than CC (Figs. 2d and 2e), whereas iWUE and Ci* were higher (Figs. 2c and 2f). Principal Component Analysis revealed that the seedlings exposed to FC were primarily grouped to growth and CO_2 compensation point (dominated by biomass, N_{leaf}, $CCP_{aci,}$ and C_i^*) on the right ellipse of PC1 (Fig. 3), while the seedlings in the CC treatment was mainly clustered in the left ellipse dominated by A_{n-t} and g_m (Fig. 3).

Features of A/C_i

The transition point (Ci-t, An-t) was lowered by the FC treatment (Fig. 4). A_{n-t} was lower in FC than in CC but the difference in C_{i-t} was not statistically significant (Table 1, Fig. 4b). Photosynthetic rate measured at growth CO_2 (A_{n-g}) was higher in FC than in CC (Fig. 4). The FC treatment increased the CO_2 compensation point estimated from A/C_i curves (CCP_{aci}) but reduced the apparent carboxylation efficiency (ACE) (Table 1, Fig. 4).

Leaf N content and concentration

Neither mass-based (N_{mass}) nor area-based (N_{area}) leaf N concentration was significantly affected by the FC treatment (Fig. 5). However, the total leaf N content per seedling (N_{leaf}) and photosynthetic N use efficiency (PNUE = A_{n-g}/N_{area}) were increased in FC (Fig. 5d).

DISCUSSION

Growth and photosynthesis acclimation

In general, a higher carboxylation capacity is a physiological mechanism to compensate for the deficient CO_2 supply under current CO_2 conditions in C3 plants and the photosynthetic capacity generally declines in response to elevated CO_2. Amur linden seedlings in this study demonstrated both morphological (e.g., total leaf area) and physiological (e.g., CCP_{aci}) acclimation to the FC treatment. The reduction in leaf-area based photosynthetic capacity in FC was accompanied by an increase in total leaf area per tree, resulting in greater seedling growth and higher nitrogen use efficiency in the FC treatment. While temperate broad-leaf tree species, e.g., *Fagus* and *Quercus,* tend to retain a significant portion of newly photosynthates in the leaf, *Tilia* species generally translocate nearly all newly synthesized photosynthates to sinks to produce new tissues and storage lipid (triacylglycerol) in wood, (Keel et al. 2007), which helps to explain the positive relationship between seedling biomass, leaf area and photosynthetic rates in response to the FC treatment. The conclusion was further corroborated by the results of the Principal Component Analysis that seedling biomass was positively associated with N_{leaf}, C_i*, and CCP_{aci}. These findings support our hypothesis that amur linden will increase photosynthate production under elevated CO_2 and warmer temperature and that the increase in photosynthate production will lead to an increase in the total leaf area and biomass. Our results are consistent with the conclusion of Smith and Keenan 2020 that elevated CO_2 increases the proportion of photosynthates used for the synthesis of new tissues and growth.

单击或点击此处输入文字。

A/C$_i$ curve patterns

A/C_i curves can be used to calculate V_{cmax} and J_{max}, and to obtain the transition point (C_{i-t}, A_{n-t}) of photosynthetic limitation from the Rubico carboxylation to RuBP regeneration , CCP_{aci}, and ACE (Fernández-Marín et al. 2020). It should be noted that photosynthetic capacity (V_{cmax} and J_{max}) is the potential maximum rate while the actual rate of photosynthesis is the portion of the

photosynthetic capacity that is realized under specific physiological and environmental conditions, such as the availability of substrates, the activation state of enzymes activation, light, temperature, etc. (Stefanski et al. 2020). Consequently, the qualities of photosynthetic acclimation may be evaluated by analyzing the varying A/C_i patterns of plants exposed to FC.

It is interesting to note that there was no significant difference in $C_{i\text{-}t}$ between the two treatments, and both were greater than the corresponding C_i ($C_{i\text{-}t} > C_{i\text{-}g}$), indicating that photosynthesis was still limited by Rubisco carboxylation under the future elevated CO_2 of 750 μmol mol^{-1} (Fig. 4b). This result is in contrast to the findings of some other studies that photosynthesis typically operates at the RuBP regeneration restriction stage ($C_{i\text{-}t} < C_{i\text{-}g}$) under elevated CO_2 (Suzuki et al. 2021). Our results suggest that the photosynthesis of amur linden may continue to be limited by V_{cmax} under elevated CO_2 levels in the foreseeable future (Kumarathunge et al. 2019). The J_{max}/V_{cmax} ratio was not altered by the FC treatment. The J_{max}/V_{cmax} ratio indicates the balance between electron transport and Rubisco capacity (Silva-Pérez et al. 2020).

The A/C_i data indicate that the FC treatment reduced ACE but increased A_n and CCP_{aci} in amur linden. This combination of changes is generally considered as a typical manifestation of a decrease in leaf-area based photosynthetic capacity (Bohley et al. 2019). The effects of FC treatment on A/C_i curves can be summarized as reduced initial slope (related to V_{cmax} and ACE), increased the actual A_n (related to J_{max}), but FC did not affect the relatively high transition point of photosynthetic limitation from Rubisco limitation to RuBP regeneration limitation ($C_{i\text{-}t}$).

It is interesting to note that the principle component analysis showed close positive relationships among the CO_2 compensation point (CCP_{aci} or C_i^*) of photosynthesis, seedling biomass, height, total leaf area, and leaf nitrogen concentration in amur linden seedlings. The CO_2 compensation point reflects the balance in resource allocation between photosynthetic and respiratory apparatuses (Walker and Cousins 2013). There are two CO_2 compensation points along the CO_2 diffusion pathway to the carboxylation site in the chloroplast that are commonly estimated: the CO_2 compensation point in the chloroplast (C_c^*) and that in the intercellular space (C_i^*). Walker and Cousins (2013) suggest that C_c^* quantifies the photorespiration production of CO_2 and the kinetic properties of Rubisco, which should be fundamental terms in photosynthetic models (Walker and Cousins 2013). The difference between C_i^* and C_a^* is affected by the

mesophyll conductance g_m. Therefore, the CO_2 compensation point estimated from the A/C_i curve may reflect the effects of multiple limitations of the photosynthetic processes (Niessen et al. 2012).

CONCLUSIONS

This study suggests that the combination of elevated CO_2 and warmer temperature as predicted for the end of the century could increase amur linden growth, especially height growth and total leaf area. Such increases can potentially further increase the shade tolerance of the species. Although photosynthetic capacity related parameters were downregulated in the FC treatment, the photosynthetic rate was higher in FC than in the CC treatment. Our results suggest that the photosynthesis of amur linden was still primarily limited by Rubisco carboxylation in seedings grown under the FC rather than shifting to RuBP regeneration limitation. RuBP regeneration limitation is generally related to a reduction in resource allocation to light harvesting and electron transport apparatus. The maintenance of this capacity in combination with an increase in total leaf area would likely boost the shade tolerance of the species in the future, particularly under dynamic light conditions under a forest canopy (Lambers and Oliveira 2019). The relatively constant C_{i-t} may have played an important role in the photosynthetic acclimation of amur linden seedlings.

References

Aasamaa K, Aphalo PJ (2017) The acclimation of *Tilia cordata* stomatal opening in response to light, and stomatal anatomy to vegetational shade and its components. Tree Physiology 37:209–219. https://doi.org/10.1093/treephys/tpw091

Ainsworth EA, Long SP (2021) 30 years of free-air carbon dioxide enrichment (FACE): What have we learned about future crop productivity and its potential for adaptation? Global Change Biology 27:27–49. https://doi.org/10.1111/gcb.15375

Apgaua DMG, Tng DYP, Forbes SJ, Ishida YF, Vogado NO, Cernusak LA, Laurance SGW (2019) Elevated temperature and CO_2 cause differential growth stimulation and drought survival responses in eucalypt species from contrasting habitats. Tree Physiology 39:1806–1820. https://doi.org/10.1093/treephys/tpz095

Baczewska-Dąbrowska AH, Dmuchowski W, Gozdowski D, Gworek B, Jozwiak A, Swiezewska E, Dąbrowski P, Suwara I (2022) The importance of prenol lipids in mitigating salt stress in the leaves of *Tilia × euchlora* trees. Trees 36:393–404. https://doi.org/10.1007/s00468-021-02214-8

Bohley K, Schröder T, Kesselmeier J, Ludwig M, Kadereit G (2019) C4-like photosynthesis and the effects of leaf senescence on C4-like physiology in *Sesuvium sesuvioides* (Aizoaceae). Jouranl of Experimental Botany 70:1553–1565. https://doi.org/10.1093/jxb/erz011

Chavan SG, Duursma RA, Tausz M, Ghannoum O (2019) Elevated CO_2 alleviates the negative impact of heat stress on wheat physiology but not on grain yield. Journal of Experimental Botany 70:6447–6459. https://doi.org/10.1093/jxb/erz386

Dang Q-L, Marfo J, Du F, Man R, Inoue S (2021) CO_2 stimulation and response mechanisms vary with light supply in boreal conifers. Journal of Plant Ecology 14:291–300. https://doi.org/10.1093/jpe/rtaa086

Dong H, Huang Z, Li W, Yu L (2023) Species-specific growth, morphological and physiological responses of *Abies faxoniana* and *Picea purpurea* under elevated temperature and CO_2. Journal of Plant Ecology 16. https://doi.org/10.1093/jpe/rtac049

Dusenge ME, Madhavji S, Way DA (2020) Contrasting acclimation responses to elevated CO_2 and warming between an evergreen and a deciduous boreal conifer. Global Change Biology 26:3639–3657. https://doi.org/10.1111/gcb.15084

Dusenge ME, Duarte AG, Way DA (2019) Plant carbon metabolism and climate change: elevated CO_2 and temperature impacts on photosynthesis, photorespiration and respiration. New Phytologist 221:32–49. https://doi.org/10.1111/nph.15283

Dusenge ME, Wittemann M, Mujawamariya M, Ntawuhiganayo EB, Zibera E, Ntirugulirwa B, Way DA, Nsabimana D, Uddling J, Wallin G (2021) Limited thermal acclimation of photosynthesis in tropical montane tree species. Global Change Biology 27:4860–4878. https://doi.org/10.1111/gcb.15790

Duursma RA (2015) Plantecophys--An R package for analysing and modelling leaf gas exchange data. PLoS One 10:e0143346. https://doi.org/10.1371/journal.pone.0143346

Fernández-Marín B, Gulías J, Figueroa CM, Iñiguez C, Clemente-Moreno MJ, Nunes-Nesi A, Fernie AR, Cavieres LA, Bravo LA, García-Plazaola JI, Gago J (2020) How do vascular plants perform photosynthesis in extreme environments? An integrative ecophysiological and biochemical story. Plant Journal 101:979–1000. https://doi.org/10.1111/tpj.14694

G.D. Farquhar, von Caemmerer, J.A. Berry (1980) A biochemical model of photosynthetic CO_2 assimilation in leaves of C3 species. Planta 149:78–90

Gardner A, Ellsworth D, Crous K, Pritchard J, Ar M (2021) Is photosynthetic enhancement sustained

through three years of elevated CO_2 exposure in 175-year old *Quercus robur*? Tree Physiology. https://doi.org/10.1093/treephys/tpab090

Helcoski R, Tepley AJ, Pederson N, McGarvey JC, Meakem V, Herrmann V, Thompson JR, Anderson-Teixeira KJ (2019) Growing season moisture drives interannual variation in woody productivity of a temperate deciduous forest. New Phytologist 223:1204–1216. https://doi.org/10.1111/nph.15906

Hu Y, Sperotto RA, Koubouris G, Stojnić S, Bellaloui N (2023) Tree ecophysiology in the context of climate change. Journal of Forest Research. 34:1–5. https://doi.org/10.1007/s11676-023-01596-4

Huang Y-L, Kao W-Y, Yeh T-F, Chang S-T (2021) Effects of growth temperature on gas exchange of *Chamaecyparis formosensis* and C. obtusa var. formosana seedlings occupying different ecological niches. Trees 35:1485–1496. https://doi.org/10.1007/s00468-021-02130-x

Kang H-I, Lee C-B, Kwon S-H, Park J-M, Kang K-S, Shim D (2021) Comparative transcriptome analysis during developmental stages of direct somatic embryogenesis in *Tilia amurensis* Rupr. Scientific Report 11:6359. https://doi.org/10.1038/s41598-021-85886-z

Keel SG, Siegwolf RTW, Jäggi M, Körner C (2007) Rapid mixing between old and new C pools in the canopy of mature forest trees. Plant Cell Environmental 30:963–972. https://doi.org/10.1111/j.1365-3040.2007.01688.x

Kim JH, Hilleary R, Seroka A, He SY (2021) Crops of the future: building a climate-resilient plant immune system. Current Opinion Plant Biology 60:101997. https://doi.org/10.1016/j.pbi.2020.101997

Kizildeniz T, Pascual I, Irigoyen JJ, Morales F (2021) Future CO_2, warming and water deficit impact white and red Tempranillo grapevine: Photosynthetic acclimation to elevated CO_2 and biomass allocation. Physiology Plant 172:1779–1794. https://doi.org/10.1111/ppl.13388

Kramer RD, Ishii HR, Carter KR, Miyazaki Y, Cavaleri MA, Araki MG, Azuma WA, Inoue Y, Hara C (2020) Predicting effects of climate change on productivity and persistence of forest trees. Ecological Research 35:562-574. DOI: 10.1111/1440-1703.12127

Kumarathunge DP, Medlyn BE, Drake JE, Rogers A, Tjoelker MG (2019) No evidence for triose phosphate limitation of light-saturated leaf photosynthesis under current atmospheric CO_2 concentration. Plant Cell Environmental 42:3241–3252. https://doi.org/10.1111/pce.13639

Kurepin LV, Stangl ZR, Ivanov AG, Bui V, Mema M, Hüner NPA, Öquist G, Way D, Hurry V (2018) Contrasting acclimation abilities of two dominant boreal conifers to elevated CO_2 and temperature. Plant Cell Environmental 41:1331–1345. https://doi.org/10.1111/pce.13158

Li L, Wang X, Manning WJ (2019) Effects of elevated CO_2 on leaf senescence, leaf nitrogen resorption, and late-season photosynthesis in *Tilia americana* L. Frontier Plant Science 10:1217. https://doi.org/10.3389/fpls.2019.01217

Liang J, Xia J, Liu L, Wan S (2013) Global patterns of the responses of leaf-level photosynthesis and respiration in terrestrial plants to experimental warming. Journal of Plant Ecology 6:437–447. https://doi.org/10.1093/jpe/rtt003

Liu J, Li Z-S, Keyimu M, Wang X, Liang H, Feng X, Gao G, Fu B (2023) Accelerated warming in the late 20th century promoted tree radial growth in the Northern Hemisphere. Journal of Plant Ecology 16. https://doi.org/10.1093/jpe/rtac077

Maxwell TL, Canarini A, Bogdanovic I, Böckle T, Martin V, Noll L, Prommer J, Séneca J, Simon E, Piepho H-P, Herndl M, Pötsch EM, Kaiser C, Richter A, Bahn M, Wanek W (2022) Contrasting drivers of belowground nitrogen cycling in a montane grassland exposed to a multifactorial global change experiment with elevated CO_2, warming, and drought. Global Change Biology 28:2425–2441. https://doi.org/10.1111/gcb.16035

Momayyezi M, Guy RD (2017) Substantial role for carbonic anhydrase in latitudinal variation in mesophyll conductance of *Populus trichocarpa* Torr. & Gray. Plant Cell Environmental 40:138–149. https://doi.org/10.1111/pce.12851

Murphy BK, Way DA (2021) Warming and elevated CO_2 alter tamarack C fluxes, growth and mortality: evidence for heat stress-related C starvation in the absence of water stress. Tree Physiology. https://doi.org/10.1093/treephys/tpab077

Niessen M, Krause K, Horst I, Staebler N, Klaus S, Gaertner S, Kebeish R, Araujo WL, Fernie AR, Peterhansel C (2012) Two alanine aminotranferases link mitochondrial glycolate oxidation to the major photorespiratory pathway in Arabidopsis and rice. Journal Experimental Botany 63:2705–2716. https://doi.org/10.1093/jxb/err453

Noyce GL, Kirwan ML, Rich RL, Megonigal JP (2019) Asynchronous nitrogen supply and demand produce nonlinear plant allocation responses to warming and elevated CO_2. Proceedings Nattional Academy of Science 116:21623–21628. https://doi.org/10.1073/pnas.1904990116

Pastore MA, Lee TD, Hobbie SE, Reich PB (2019) Strong photosynthetic acclimation and enhanced water-use efficiency in grassland functional groups persist over 21 years of CO_2 enrichment, independent of nitrogen supply. Global Change Biology 25:3031–3044. https://doi.org/10.1111/gcb.14714

Peter CH, Francesco L, Di Giorgio M, Thomas DS (1992) Theoretical Considerations when Estimating the Mesophyll Conductance to CO_2 Flux Analysis of the Response of Photosysthesis to CO2. Plant physiology 98:1429–1436

Raizada P, Singh A, Raghubanshi AS (2009) Comparative response of seedlings of selected native dry tropical and alien invasive species to CO_2 enrichment. Journal of Plant Ecology 2:69–75. https://doi.org/10.1093/jpe/rtp006

Silva-Pérez V, Faveri J de, Molero G, Deery DM, Condon AG, Reynolds MP, Evans JR, Furbank RT (2020) Genetic variation for photosynthetic capacity and efficiency in spring wheat. Journal of Experimental Botany 71:2299–2311. https://doi.org/10.1093/jxb/erz439

Smith NG, Keenan TF (2020) Mechanisms underlying leaf photosynthetic acclimation to warming and elevated CO_2 as inferred from least-cost optimality theory. Global Change Biology 26:5202–5216. https://doi.org/10.1111/gcb.15212

Smith AR, Lukac M, Hood R, Healey JR, Miglietta F, Godbold DL (2013) Elevated CO_2 enrichment induces a differential biomass response in a mixed species temperate forest plantation. New Phytologist 198:156–168. https://doi.org/10.1111/nph.12136

Stefanski A, Bermudez R, Sendall KM, Montgomery RA, Reich PB (2020) Surprising lack of sensitivity of biochemical limitation of photosynthesis of nine tree species to open-air experimental warming and reduced rainfall in a southern boreal forest. Global Change Biology 26:746–759. https://doi.org/10.1111/gcb.14805

Suzuki Y, Ishiyama K, Sugawara M, Suzuki Y, Kondo E, Takegahara-Tamakawa Y, Yoon D-K, Suganami M, Wada S, Miyake C, Makino A (2021) Overproduction of Chloroplast Glyceraldehyde-3-Phosphate Dehydrogenase Improves Photosynthesis Slightly under Elevated CO_2 Conditions in Rice. Plant Cell Physiology 62:156–165. https://doi.org/10.1093/pcp/pcaa149

Walker BJ, Cousins AB (2013) Influence of temperature on measurements of the CO_2 compensation point: differences between the Laisk and O_2-exchange methods. Journal of Experimental Botany 64:1893–1905. https://doi.org/10.1093/jxb/ert058

Wang L, Zheng J, Wang G, Dang Q-L (2022) Increased leaf area compensated photosynthetic downregulation in response to elevated CO_2 and warming in white birch. Canadian Journal of Forest

Research. 52:1176–1185. https://doi.org/10.1139/cjfr-2022-0076

Way DA, Oren R, Kroner Y (2015) The space-time continuum: the effects of elevated CO_2 and temperature on trees and the importance of scaling. Plant Cell Environmental 38:991–1007. https://doi.org/10.1111/pce.12527

Xu H, Wang H, Prentice IC, Harrison SP, Wang G, Sun X (2021) Predictability of leaf traits with climate and elevation: a case study in Gongga Mountain, China. Tree Physiology 41:1336–1352. https://doi.org/10.1093/treephys/tpab003

Zhang P, Lü X-T, Li M-H, Wu T, Jin G (2022) N limitation increases along a temperate forest succession: evidences from leaf stoichiometry and nutrient resorption. Journal of Plant Ecology 15:1021–1035. https://doi.org/10.1093/jpe/rtac017

Zheng W, Li R, Yang Q, Zhang W, Huang K, Guan X, Chen L, Yu X, Wang Q, Wang S (2023) Allocation patterns of nonstructural carbohydrates in response to CO_2 elevation and nitrogen deposition in *Cunninghamia lanceolata* saplings. Journal of Forest Research. 34:87–98. https://doi.org/10.1007/s11676-022-01533-x

Table

Table 1 ANOVA P-values for the effects of CO_2 and Temperature combination (CC vs. FC) on the growth, and photosynthesis of amur linden seedlings. Significant effects ($P \leq 0.05$) are shown in bold.

Variables	F	P-value	Variables	F	P-value
Biomass	56.632	**< 0.001**	V_{cmax}	18.156	**0. 002**
RMR	0.539	0.482	J_{max}	6.672	**0.03**
SMR	16.787	**0.003**	J_{max}/V_{cmax}	0.002	0.964
LMR	0.112	0.746	C_{i-t}	0.754	0.408
Leaf area	35.677	**< 0.001**	A_{n-t}	27.195	**< 0.001**
Hight	28.965	**< 0.001**	g_m	35.404	**< 0.001**
A_{n-g}	6.569	**0.028**	R_d	7.498	**0.023**
N_{area}	2.181	0.174	C_i*	49.68	**< 0.001**
N_{mass}	0.014	0.907	ACE	5.903	**0.038**
N_{leaf}	53.273	**< 0.001**	$CCPaci$	29.082	**< 0.001**
PNUE	10.6	**0.01**	$iWUE$	113.1	**< 0.001**

Note: RMR: root mass ratio; SMR: stem mass ratio; LMR: leaf mass ratio; N_{area}: leaf N per unit area; N_{mass}: leaf N concentration; N_{leaf}: total N of the whole-plant leaf; PNUE: photosynthetic nitrogen use efficiency; C_{i-t}: intercellular $[CO_2]$ at the transition point (C_{i-t}, A_{n-t}) between Rubisco limitation and RuBP regeneration limitation based on A/C_i curve; A_{n-t}: net photosynthesis rate at C_{i-t}; R_d: daytime respiration; C_i*: intercellular CO_2 compensation point; ACE: apparent carboxylation efficiency; CCP_{aci}: CO_2 compensation point from A/C_i curve; A_{n-g}: net photosynthesis rate at corresponding growth C_a.

Figure Captions

Figure 1: Effects of CO_2 &Temperature combination treatment (CC vs. FC) on biomass (a), height (b), leaf area (c), and stem mass ratio (d). Means ($\pm$ SE, n=6) with different letters were different from each other ($p \leq 0.05$).
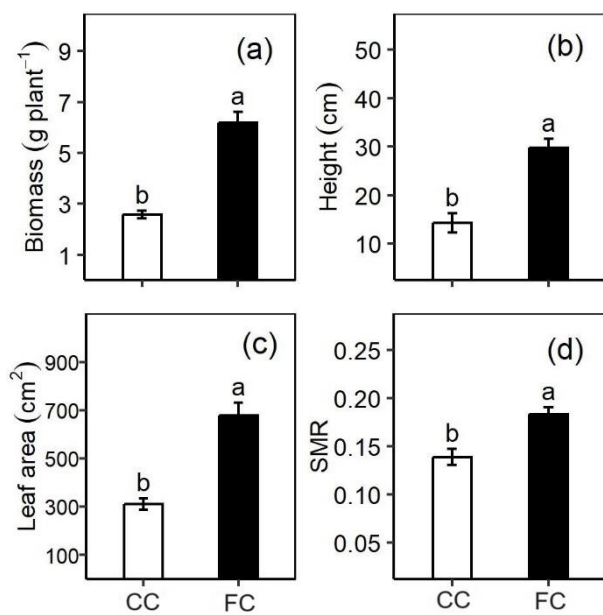
Figure 2: Effects of CO_2 and Temperature combination treatment on V_{cmax}: maximum rate of Rubisco carboxylation (a), J_{max}: maximum rate of photosynthetic electron transport rate (b), $iWUE$: instantaneous water use efficiency with instantaneous photosynthetic (c), g_m: mesophyll conductance (d), R_d: daytime respiration (e), C_i*: intercellular CO_2 compensation point (f). Means ($\pm$ SE, n=6) with different letters are different from each other ($p \leq 0.05$).

Figure 3: Principal Component Analysis (PCA, using FactoMineR package in R) of growth and photosynthetic parameters with significant treatment effects (CC vs. FC). The polygons indicate treatment clustering. Abbreviations: J_{max} (maximum of photosynthetic electron transport rate), V_{cmax}: maximum rate of ribulose-1,5-bisphosphate carboxylation), R_d (daytime respiration), g_m (mesophyll conductance), A_{n-t} (net photosynthesis rate at the transition point between Rubisco limitation and RuBP regeneration limitation based on A/C_i curve), N_{leaf}: total N of the whole-plant leaf, CCP_{aci} (C_i compensation point from A/C_i curve), C_i* (intercellular CO_2 compensation point). See Table 1 for other explanations.

Figure 4: A/C_i curves of *Tilia* seedlings grown either under CC (a) or FC (b). Each point in the plots represents the average of six sample seedlings. The measurements of all the sample seedlings (3 seedlings per replicate, 2 replicates per treatment) were used to generate the curves to better represent the average performance of all the seedlings in the treatment and the variations among seedlings were represented by error bars in the figure. The open circle at the crossing point in each plot denotes the transition point (C_{i-t}, A_{n-t}) from the Rubisco limitation to the RuBP limitation. C_{i-g} and A_{n-g} represent values measured at growth CO_2 concentration; ACE: apparent carboxylation efficiency derived from the initial slope of the A/C_i curve; CCP_{aci}: CO_2 compensation point derived from A/C_i curve, i.e., C_i when A_n was zero. Both ACE and CCP_{aci} were different between C and F ($p \leq 0.05$, Table 1). Ac = V_{cmax} limited photosynthetic rate; Aj = J_{max} limited rate.
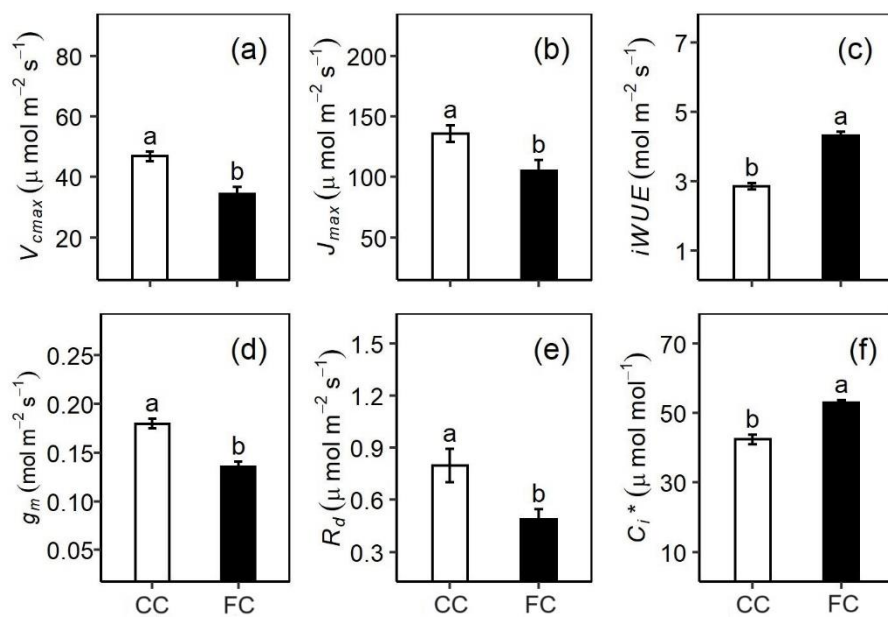
Figure 5: Effects of CO_2 and Temperature combination (CC vs. FC) on leaf mass (N_{mass}, a), leaf area (N_{area}, b), leaf of the whole plant (N_{leaf}, c) of N concentration, and photosynthetic nitrogen use efficiency (PNUE, d). Means ($\pm$ SEM, n=6) with different letters are different from each other ($p \leq 0.05$). See Table 1 for other explanations.
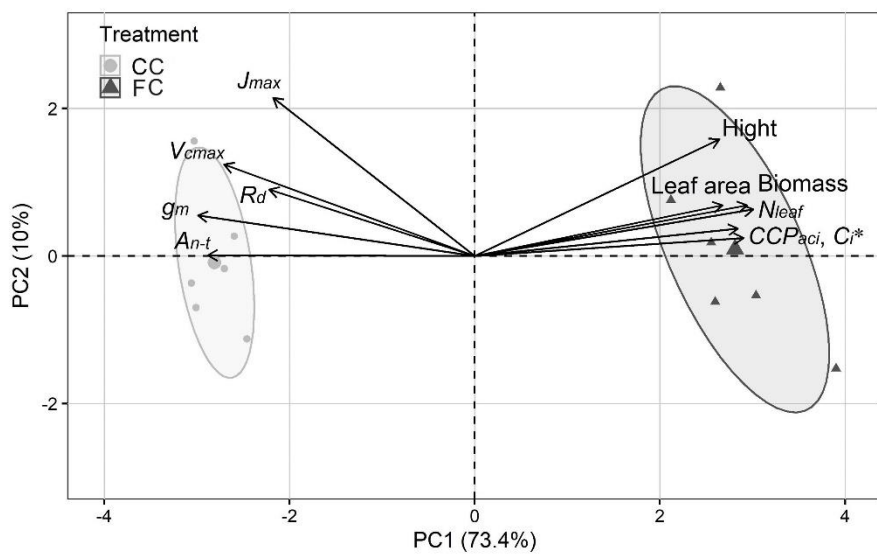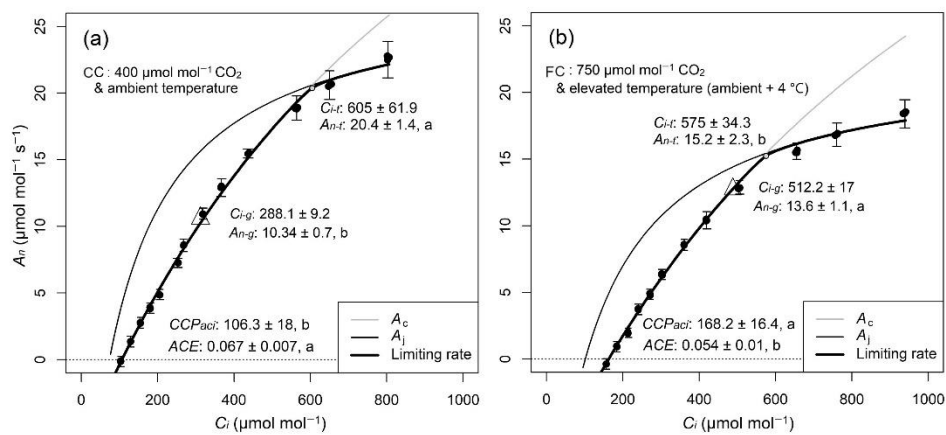
Figure 1

Figure 2

Figure 3

Figure 4

(a) CC : 400 μmol mol⁻¹ CO₂ & ambient temperature

C_{i-t}: 605 ± 61.9
A_{n-t}: 20.4 ± 1.4, a

C_{i-g}: 288.1 ± 9.2
A_{n-g}: 10.34 ± 0.7, b

CCP_{aci}: 106.3 ± 18, b
ACE: 0.067 ± 0.007, a

A_c
A_j
Limiting rate

(b) FC : 750 μmol mol⁻¹ CO₂ & elevated temperature (ambient + 4 °C)

C_{i-t}: 575 ± 34.3
A_{n-t}: 15.2 ± 2.3, b

C_{i-g}: 512.2 ± 17
A_{n-g}: 13.6 ± 1.1, a

CCP_{aci}: 168.2 ± 16.4, a
ACE: 0.054 ± 0.01, b

A_c
A_j
Limiting rate

Figure 5